Preprints of the 19th World Congress
The International Federation of Automatic Control
Cape Town, South Africa. August 24-29, 2014

Motion planning and control of formations of micro aerial vehicles

Martin Saska* **Zdenek Kasl*** **Libor Přeučil***

* *Czech Technical University in Prague, Department of Cybernetics*
e-mail: saskam1@fel.cvut.cz, kaslzden@fel.cvut.cz,
preucil@labe.felk.cvut.cz

Abstract: A model predictive control based algorithm for maintenance of leader-follower formations of micro-scale aerial vehicles is proposed in this paper. The approach is designed for stabilization of teams of unmanned quadrotor helicopters and for their motion planning into a distant target region. The presented method of the model predictive control with a planning horizon enables integration of an obstacle avoidance function into the local control of the formation as well as into the global plan of formation movement. Deployment of the method in real-world scenarios, with particular interest in failure recovery and inter-vehicle avoidance, is verified in various simulations.

Keywords: Aircraft control, micro unmanned vehicles, mobile robots, helicopter control, model predictive control, obstacle avoidance, formation stabilization, trajectory planning

1. INTRODUCTION

Motion coordination of large teams of Micro Aerial Vehicles (MAVs) requires precise relative localization, which is nowadays usually provided by external motion capture systems (Kumar and Michael, 2012). However, in most of the real-world missions (such as search and rescue or reconnaissance), multi-robot systems have to be cooperatively deployed in large areas in a short time and may not rely on such a pre-installed global localization infrastructure. Worldwide available systems (like GPS) lack the required precision for compact teams of small robots, and lose reliability in urban and indoor environments.

We present a formation driving Model Predictive Control (MPC) based approach adapted for onboard visual relative localization of unmanned helicopters (quadrotors). In the investigated scenario, the formation of multiple MAVs has to reach a desired target region in a complex environment with obstacles, while keeping predefined relative positions between the robots. The desired shape of the formation can be temporarily changed only if it is enforced by environmental constraints (e.g. in narrow passages).

In this paper, we rely on a leader-follower method, where the team of robots is stabilized by sharing knowledge of the leader's position within the formation. See work of Das et al. (2003) for the basic principles of the leader-follower approach, and see papers of Sira-Ramirez and Castro-Linares (2010); Min and Papanikolopoulos (2012) and references reported therein for the state-of-the-art. Recently, research endeavor in the formation driving community has been aimed mainly at tasks of formation stabilization (Liu and Jia, 2012) and formation following a predefined path (Sira-Ramirez and Castro-Linares, 2010).

⋆ The work was supported by the Grant Agency of the Czech Republic under grant no. P103-12/P756.

The state-of-the-art of approaches designed for MAVs may represent works of No et al. (2011) and Liu et al. (2011). The formation stabilization and desired shape keeping are treated as a dynamic 3-D tracking problem via a cascade-type guidance law in (No et al., 2011). Liu et al. (2011) propose an on-line embedded solution of a leader-follower approach for stabilizing helicopter formations using a nonlinear model predictive control. This work shows that the computational power of microprocessors available onboard unmanned helicopters enables the employment of MPC techniques also for the formation control of these highly dynamic systems, as is proposed in this paper. Recently, researchers have taken advantage of MPC to respond to changes in a dynamic environment, again mainly in tasks including path tracking and formation stabilization (Chao et al., 2012; Defoort, 2010). Chao et al. (2012) propose a new cost penalty into MPC optimization. It guarantees the obstacle avoidance with a priority strategy employed for ensuring the inter-vehicle collision avoidance. A decentralized receding horizon motion planner is developed by Defoort (2010) to coordinate robots using neighbour-independent planning.

In our approach, we go beyond these works in several aspects. We apply the MPC technique for the stabilization of followers in the desired positions behind the leader, as well as for the trajectory planning into a desired goal area with obstacle avoidance ability. We do not rely on following a given trajectory, as in most of the state-of-the-art methods. The global trajectory planning is directly integrated into the formation control mechanism. This is necessary for finding a feasible solution for the relative visual localization of team members, where the constraints of direct visibility have to be satisfied. We propose a new MPC concept combining both, the trajectory planning into the desired goal region and the immediate control of the formation in a single optimization process. The proposed method is an extension of our previous work Saska

et al. (2013), where a formation driving of ground robots were investigated. The method can continuously respond to changes in the vicinity, while keeping the cohesion of the immediate control inputs with the directions of movement of the MAV formation in the future.

2. PRELIMINARIES

2.1 Model

The quadrotor vehicle model with four identical propellers located at vertices of a square is used in the proposed model predictive control. Each of the propellers l generates a thrust f_i^l along axis of i-th MAV in the formation. Symbol $i \in \{L, 1, \ldots, n_r\}$ denotes the leader L and n_r followers. For each MAV, we consider an inertial reference frame and a body-fixed frame with origin located at the center of mass of the MAV. The relative position of the i-th frame at time t is defined by the location of the center of mass $x_i(t) \in \mathbb{R}^3$ in the inertial frame and by the rotation matrix $R_i(t) \in \mathbb{R}^{3\times3}$ from the body-fixed frame to the inertial frame. The notation $x_i := x_i(t)$, $R_i := R_i(t)$ etc. is used in the paper for simplification, if the time, when the variable is obtained, does not need to be specified.

The motion model of MAVs is used according to Lee et al. (2010) as

$$\begin{aligned} \dot{x_i} &= v_i, \\ m_i \dot{v_i} &= m_i g e_3 - f_i R_i e_3, \\ \dot{R_i} &= R_i \hat{\Omega}_i, \\ J_i \dot{\Omega}_i + \Omega_i \times J_i \Omega_i &= M_i, \end{aligned} \tag{1}$$

where $v_i \in \mathbb{R}^3$ is the velocity of center of mass in the inertial frame, $m_i \in \mathbb{R}$ is the mass of i-th MAV, $\Omega_i \in \mathbb{R}^3$ is the angular velocity in the body-fixed frame, and $J_i \in \mathbb{R}^3$ is the inertia matrix with respect to the body-fixed frame. The hat symbol $\hat{\cdot}$ is defined by the condition $\hat{a}b = a \times b$ for all $a, b \in \mathbb{R}^3$, g is the gravity acceleration, and vectors $\mathbf{e}_1, \mathbf{e}_2, \mathbf{e}_3 \in \mathbb{R}^3$ are columns of the identity matrix $\mathbf{E}$, i.e. $\mathbf{e}_1 = [1\ 0\ 0]^T$, $\mathbf{e}_2 = [0\ 1\ 0]^T$ and $\mathbf{e}_3 = [0\ 0\ 1]^T$. $M_i \in \mathbb{R}^3$ is the moment along axes of the body-fixed frame and $f_i \in \mathbb{R}$ is the thrust. The total thrust, $f_i = \sum_{l=1}^{4} f_i^l$, acts in the direction of the axis of the body-fixed frame which is orthogonal to the plane defined by the centres of the four propellers. Let us assume that the environment of the robots contains a finite number n_0 of compact obstacles $o_l \in \mathcal{O}$, $l \in \{1, \ldots, n_0\}$.

2.2 Leader-follower approach

The shape of the entire formation is maintained with a leader-follower technique based on the notation presented in (Barfoot and Clark, 2004). In this subsection, we extend the approach of distribution of desired positions of followers, which was designed by Barfoot and Clark (2004) for formations of ground vehicles in a planar environment, into 3D space, as it is necessary for the stabilization of formations of MAVs investigated in this paper.

In the algorithm, followers follow the trajectory of the leader in distances defined in the p, q, h curvilinear

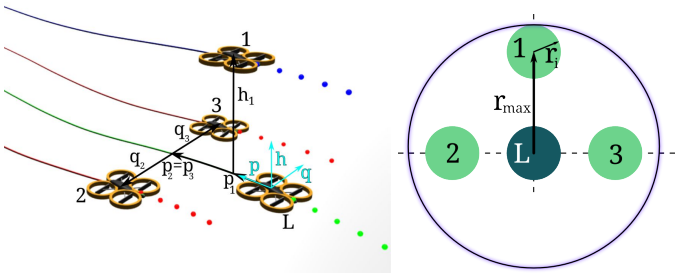

(a) (b)

Fig. 1. (a) The desired shape of the formation described in curvilinear coordinates. (b) Representation of the formation applied in the obstacle avoidance function. The projection of the formation is realized by setting p coordinates equal to zero for all followers.

coordinate system, as visualized in Fig.1(a). The position of each follower i is uniquely determined: 1) by states $x_L(t_{p_i})$ in the *travelled distance* p_i from the actual position of the leader along its trajectory, 2) by the *offset distance* q_i from the trajectory in the perpendicular direction and, 3) by the elevation h_i above the trajectory. t_{p_i} denotes the time when the virtual leader was at the *travelled distance* p_i behind the actual position.

To convert the state of the followers in curvilinear coordinates to a state in Cartesian coordinates at time t, the following equations can be applied:

$$\begin{aligned} x_i(t) &= x_L(t_{p_i}) + \begin{pmatrix} -q_i \sin(\phi_L(t_{p_i})) \\ q_i \cos(\phi_L(t_{p_i})) \\ h_i \end{pmatrix}, \\ \phi_i(t) &= \phi_L(t_{p_i}), \end{aligned} \tag{2}$$

where $x_L(t_{p_i})$ is the position of the leader at time t_{p_i} and $\phi_L(t_{p_i})$ is Yaw angle of the leader at time t_{p_i}. Control (and planning) of horizontal and vertical velocities is decoupled in the method.

3. TRAJECTORY PLANNING AND FORMATION STABILIZATION

3.1 Predictive control for leader

Commonly used MPC based methods solve a finite horizon optimization control problem for the system represented by the kinematic model from the current states over the time interval $\langle t_0, t_0 + N\Delta t\rangle$. This interval is known as the *control horizon*. The sampling time Δt inbetween the N transition points is constant in this interval. We have extended this standard scheme with an additional time interval with M transition points. This *planning horizon*, which is crucial for incorporation of requirements given by the visual relative localization, is used for planning the trajectory of the leader into the desired target region, which is defined as a ball with radius r_{S_F} and center C_{S_F}. The time difference between the M transition points is variable in this time interval. This planning algorithm respects constraints given by the desired shape of the formation, by the relative localization and by the kinematics of the followers. In this approach, we solve in a single optimization step two problems that are usually separated:

1) The formation trajectory planning which provides a long-term plan to the target location. 2) The computation of the immediate control sequences responding to local workspace of robots.

The trajectory encoded into a vector of constant control inputs at time t is used as the optimization vector $X_L(t) = [{}^{\nu}v_{L,1},\ {}^{\tau}v_{L,1},\ k_{L,1},\ \dots\ ,\ {}^{\nu}v_{L,N},\ {}^{\tau}v_{L,N},\ k_{L,N},\ {}^{\nu}v_{L,N+1},\ {}^{\tau}v_{L,N+1},\ k_{L,N+1},\ \delta_{L,N+1},\ \dots,\ {}^{\nu}v_{L,N+M},\ {}^{\tau}v_{L,N+M},\ k_{L,N+M},\ \delta_{L,N+M}]$, which includes both, the local and global motion planning. The vector $X_L(\cdot)$ consists of the vertical velocity ${}^{\nu}v_{L,\cdot}\,[\mathrm{m{\cdot}s^{-1}}]$, the horizontal velocity ${}^{\tau}v_{L,\cdot}\,[\mathrm{m{\cdot}s^{-1}}]$, the curvature $k_{L,\cdot}\,[\mathrm{m^{-1}}]$, and the length of the time interval $\delta_{L,\cdot}\,[\mathrm{s}]$. The vertical velocity is given by equation ${}^{\nu}v_L = {v_L}^T e_3$. The horizontal velocity is given by composition of the x and y components of the velocity vector v_L as ${}^{\tau}v_L = {v_L}^T e_1 \cos(\phi_L) + {v_L}^T e_2 \sin(\phi_L)$. The curvature $k_{L,\cdot}$ of the trajectory followed by the leader is constant within each control segment and may vary along the whole trajectory. The time interval $\delta_{L,j}$ is constant if $j \in \{1 \dots N\}$ and becomes variable if $j \in \{N+1 \dots N+M\}$. The constant time interval is denoted as Δt and set as $\delta_{L,j} := \Delta t = 0.1s$, $j \in \{1 \dots N\}$, in the experiments. The control inputs ${}^{\tau}v_{L,j}$, ${}^{\nu}v_{L,j}$ and $k_{L,j}$ are constant over given time interval $\delta_{L,j}, j \in \{1 \dots N+M\}$ in the trajectory described by the optimization vector $X_L(\cdot)$.

The leader's control problem with the obstacle avoidance ability can then be transformed to minimization of the multi-objective cost function $F_L(X_L(\cdot), \mathcal{O})$ subject to set of constraints. The chosen components of the cost function affect desired quality of the obtained solution (distance to obstacles, time to reach the goal, smoothness of movement), and also stability and convergence of the optimization process. The objective function is given as a weighted sum of all these components, which are described bellow. Weights are provided by the user based on particular application that determines the importance of a particular property of the solution.

In each evaluation of the cost function, the states of the controlled plant are predicted using the MAV model stated in equation (1). Such a simulation of behaviour of the plant shows a response to the control inputs obtained from the optimization vector. The model prediction also includes the transient response to suddenly changing control inputs between each two consecutive time intervals, where the control is constant. It decreases the deviation of the real system from the obtained plan, which is important for the convergence of the system into the desired equilibrium.

Obstacle proximity penalisation prevents the formation from collisions with obstacles as follows:

$$F_{L,obst}(X_L(\cdot),\mathcal{O}) = \sum_{l=1}^{n_o} \left(\min \left\{ 0,\ \frac{dist(X_L(\cdot), o_l) - r_{s,L}}{dist(X_L(\cdot), o_l) - r_{a,L}} \right\} \right)^2. \quad (3)$$

The value of this obstacle avoidance function (originally described in Stipanović et al. (2007)) is zero, if all formation members following the leader in their desired positions within the formation are in a safe distance from all obstacles. This means that the distance $dist(X_L(\cdot), o_l)$ between the trajectory of the leader and the obstacle o_l is for all obstacles greater than $r_{s,L}$ and $r_{s,L} > r_{max} + r$, where r is radius of a sphere representing MAVs and r_{max} is radius of the formation defined in Fig. 1(b). The value of $F_{L,obst}(X_L(\cdot), \mathcal{O})$ increases if an obstacle approaches into the sphere defined by the safety radius $r_{s,L}$. The representation of the entire formation as a sphere is crucial for the visual relative localization of the team members. It ensures that the direct visibility between the robots will not be broken by an obstacle located among them. Radius $r_{a,L}$ is the critical avoidance radius. As the distance between the robots and obstacles reaches $r_{a,L}$, the value of function (3) goes to infinity. The condition $r_{a,L} < r_{s,L}$ has to be satisfied. The critical avoidance radius can be for some applications shorter than $r_{max} + r$. This setting allows the system to find a trajectory, which is feasible for the formation but only at the cost of a temporary shrinking of its shape (e.g. in a narrow corridor as shown in Fig. 2). The deviation of followers from their desired positions within the formation is realised in the trajectory following mechanism with the obstacle avoidance function, which is described in the next section. It is important to emphasize that these solutions are penalized by the $F_{L,obst}(X_L(\cdot), \mathcal{O})$ component of the cost function and therefore solutions without the necessity to change the shape of the formation are preferred by the system if they correspond with the minimum of the multi-objective cost function.

Time of flight penalization is based on an estimation of the total time required for reaching the desired target region. The time needed for realization of the first part of the trajectory is constant since the fixed number of transition points N is distributed in the control horizon with the constant frequency. Therefore, only the planning horizon has to be considered in the penalization as follows:

$$F_{L,time}(X_L(\cdot)) = \sum_{j=N+1}^{N+M} \delta_{L,j}. \quad (4)$$

Penalization of movement oscillations has to prevent the system from undesired sudden changes in robot's control inputs, which may occur if only a suboptimal solution of the optimization is found due to limited computational time. This third component of the proposed cost function is applied to achieve a smooth formation movement as follows:

$$F_{L,osc}(X_L(\cdot)) = \sum_{j=1}^{N+M} (k_{L,j} - \bar{k}_L)^2 + (v_{L,j} - \bar{v}_L)^2, \quad (5)$$

where $\bar{k}_L$ and $\bar{v}_L$ denote mean values of curvature and velocity in the particular solution.

Obstacle proximity constraint is crucial for ensuring that the distance between the trajectory and obstacles is always more than the radius $r_{a,L}$. If an obstacle appears within the radius $r_{a,L}$, the obstacle proximity penalisation does not work properly and therefore the obstacle proximity constraint has to be applied as follows:

$$C_{L,obst}(X_L(\cdot), \mathcal{O}) := r_{a,L} - \min_{l=1\cdots n_o} (dist(X_L(\cdot), o_l)) \leq 0. \quad (6)$$

Distance to target constraint is crucial for the stability and convergence of the formation driving process. The aim of the constraint is to ensure that the plan for the leader enters the desired target region. Solutions that do not satisfy the following equation are considered as infeasible and the convergence into the target region cannot be guaranteed in this case. The *distance to target constraint* depends on the distance of the trajectory of the leader into the target region (with radius r_{S_F} and center C_{S_F}) as follows:

$$C_{L,S_F}(X_L(\cdot), S_F) := dist(X_L(\cdot), C_{S_F}) - r_{S_F} \leq 0. \quad (7)$$

Control inputs constraints have to be applied since the control and planning approach for the leader must respect constraints given by its mechanical capabilities, but also the constraints of the guided formation, which are usually predominant. The *control inputs constraints* are then applied as follows:

$$C_{L,control}(X_L(\cdot)) := \begin{pmatrix} {}^{\nu}v_{L,j} - {}^{\nu}v_{L,max} \\ {}^{\nu}v_{L,min} - {}^{\nu}v_{L,j} \\ {}^{\tau}v_{L,j} - {}^{\tau}v_{L,max} \\ {}^{\tau}v_{L,min} - {}^{\tau}v_{L,j} \\ k_{L,j} - k_{L,max} \\ k_{L,min} - k_{L,j} \\ -\delta_{L,j} \end{pmatrix} \leq 0, \quad (8)$$

where $j \in \{1 \dots N+M\}$ for ${}^{\nu}v_{L,j}$, ${}^{\tau}v_{L,j}$, and $k_{L,j}$ and $j \in \{N+1 \dots N+M\}$ for $\delta_{L,j}$.

The admissible control set for the leader can be determined by applying the leader-follower approach and limits $k_{i,max}$, ${}^{\tau}v_{i,max}$, ${}^{\tau}v_{i,min}$, ${}^{\nu}v_{i,max}$ and ${}^{\nu}v_{i,min}$ on control inputs of each of the followers. These restrictions must be applied to satisfy different values for the curvature and the speed of the robots in different positions within the formation. Intuitively, the robot following the inner track during turning goes more slowly but with a bigger curvature than the robot further from the center of the turning.

3.2 Predictive control for followers

The trajectory of the leader obtained as a result of the algorithm described in the previous section needs to be transformed for each of the following vehicles using the transformation in equation (2). The obtained sequences of the desired states are used for the trajectory tracking algorithm with the obstacle avoidance function for each of the followers. It enables responses to events that occur in the environment behind the actual position of the leader, and to an incorrect movement of a neighbor in the formation. Similarly as for the leader, the trajectory is encoded into a vector of constant control inputs and it is used as the optimization vector $X_i(\cdot) = [{}^{\nu}v_{i,1}, {}^{\tau}v_{i,1}, k_{i,1}, \dots, {}^{\nu}v_{i,N}, {}^{\tau}v_{i,N}, k_{L,N}]$ for i-th follower. The vertical velocity ${}^{\nu}v_{i,\cdot}$ [m·s^{-1}], the horizontal velocity ${}^{\tau}v_{i,\cdot}$ [m·s^{-1}] and the curvature $k_{i,\cdot}$ [m^{-1}] are constant over the constant time interval Δt, in the trajectory described by the optimization vector $X_i(\cdot)$. The discrete-time trajectory tracking for each follower is again transformed to a minimization of the multi-objective cost function $F_i(X_i(\cdot), X_L^{\circ}, \mathcal{O})$ subject to set of constraints. [1] The function $F_i(\cdot)$ is again given as a weighted sum of several components with weights provided by the user based on particular application.

Obstacle proximity penalisation is employed for avoiding collisions with dynamic and later appearing obstacles that could not be detected by the leader. Besides, it acts as a failure tolerance mechanism as it enables avoiding collisions with other team members deviating from their desired positions within the formation:

$$F_{i,obst}(X_i(\cdot), \mathcal{O}) = \sum_{l=1}^{n_o} \left(\min \left\{ 0, \frac{dist(X_i(\cdot), o_l) - r_{s,i}}{dist(X_i(\cdot), o_l) - r_{a,i}} \right\} \right)^2 + \sum_{j \in \bar{n}_n} \left(\min \left\{ 0, \frac{d_{i,j}(X_i(\cdot), X_j^{\circ}) - r_s}{d_{i,j}(X_i(\cdot), X_j^{\circ}) - r_a} \right\} \right)^2. \quad (9)$$

The first part of the obstacle proximity penalisation is similar to the equation (3) except the size of detection and avoidance safety zones that are significantly smaller and do not depend on the shape of the formation. The second component is the sum of the avoidance functions in which the other members of the team are considered also as dynamic obstacles. This part protects the robots in the case of unexpected behaviour of defective neighbours (see Fig. 4). Function $d_{i,j}(X_i(\cdot), X_j^{\circ})$ returns the minimal distance between the planned trajectory of follower i and the actually used plan of other followers $j \in \bar{n}_n$, where $\bar{n}_n = \{1, \dots, i-1, i+1, \dots, n_r\}$.

Penalisation of deviation from desired state is the crucial component for the tracking of the leader's trajectory. It penalizes growing euclidean distance between the desired positions ${}^{d}x_{i,j}$, $j \in \{1 \dots N\}$, obtained from the actual leader's trajectory X_L°, and the positions of the i-th follower in the plan being evaluated. Additionally, a penalization of differences between the desired Yaw angles ${}^{d}\phi_{i,j}$, $j \in \{1 \dots N\}$, and the actual Yaw of follower i is included as follows:

$$F_{i,dev}(X_i(\cdot), X_L^{\circ}) = \sum_{j=1}^{N} \left({}^{d}x_{i,j} - x_j \right)^2 + \sum_{j=1}^{N} \left({}^{d}\phi_{i,j} - \phi_j \right)^2. \quad (10)$$

Penalization of movement oscillations are used similarly as for the leader planning:

$$F_{i,osc}(X_i(\cdot)) = \sum_{j=1}^{N} (k_{i,j} - \bar{k}_i)^2 + (v_{i,j} - \bar{v}_i)^2, \quad (11)$$

Obstacle proximity constraint is employed in the same way as it was shown for the leader.

Control inputs constraints are used as follows:

[1] Results of the optimization process used for the formation stabilization and control are denoted with ()° symbol in this paper.

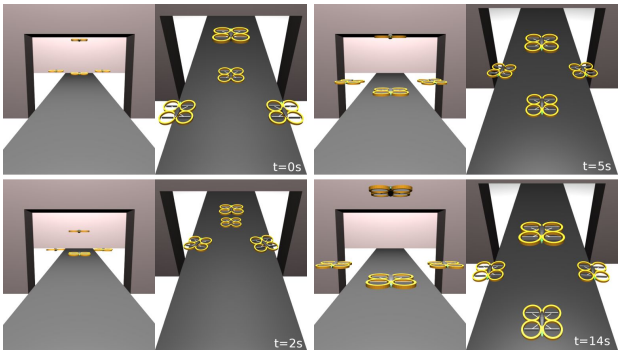

Fig. 2. Formation changing its shape in order to fly through a door. 2 snapshots with front and rear-top views are shown in the left column and 2 snapshots with front and front-top views are in the right.

$$C_{i,control}(X_L(\cdot)) := \begin{pmatrix} {}^{\nu}v_{i,j} - {}^{\nu}v_{i,max} \\ {}^{\nu}v_{i,min} - {}^{\nu}v_{i,j} \\ {}^{\tau}v_{i,j} - {}^{\tau}v_{i,max} \\ {}^{\tau}v_{i,min} - {}^{\tau}v_{i,j} \\ |k_{i,j}| - k_{i,max} \end{pmatrix} \leq 0, \qquad (12)$$

where $j \in \{1 \dots N\}$.

4. EXPERIMENTAL EVALUATION

The proposed method has been verified by various simulations and experiments with the parameters set as follows: $M = 6$, $N = 8$, $n = 2$, $\Delta t = 0.1$s. The MAV model was used with constants $m = 4.34\,\text{kg}$ and $\mathbf{J} = \begin{bmatrix} 0.0820 & 0 & 0 \\ 0 & 0.0845 & 0 \\ 0 & 0 & 0.1377 \end{bmatrix}$ kg·m^2 for all robots.

4.1 Simulations of formation movement

The first simulation aims at verification of ability of the method to control the formation through a narrow passage (e.g. a door or a window) via changing its shape, which is enforced by the obstacles. In Fig. 2, the shape of the formation is autonomously contracted. It enables flying through the door and then restoring back the desired shape of the formation. The progress of values of objective functions of followers that are forced to leave their desired positions is shown in Fig. 3. The values of the objective function increase in proximity of obstacles and as the robots are leaving their desired positions. Then the value of the objective function decreases back to zero, as the followers reach their desired position in the formation.

The fault tolerance and recovery of the proposed method is verified in the second simulation. In the experimental setup, a failure of one of the followers is simulated. Robot 2 in Fig. 4 is not capable of following the leader's trajectory and it is slowly loosing its altitude. The second follower is flying behind the faulty one and it starts its avoiding manoeuvre as a reaction on the growth of its objective function. Firstly, it decreases its speed, in order to increase the distance from the faulty follower. Since this behavior is insufficient, it autonomously performs the fly around manoeuvre as a result of the optimization process

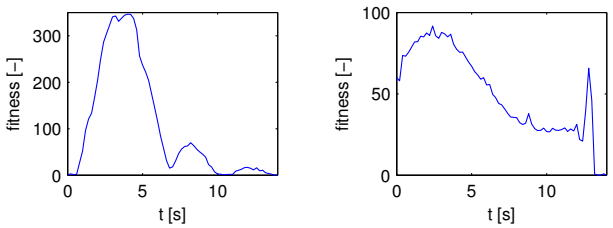

(a) Objective function of the follower flying on the left side. (b) Objective function of the follower flying above the formation.

Fig. 3. Progress of values of the objective functions from experiment in Fig. 2.

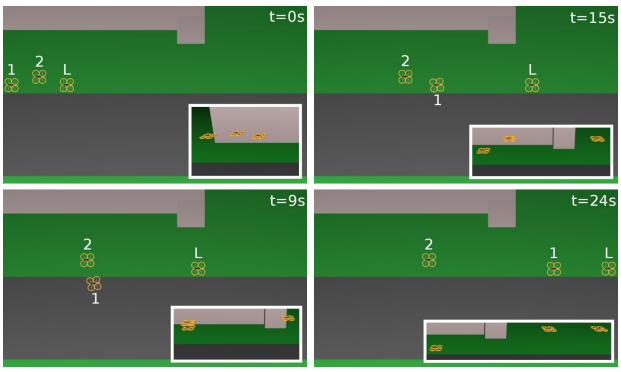

Fig. 4. Follower 1 avoiding collision with faulty follower 2.

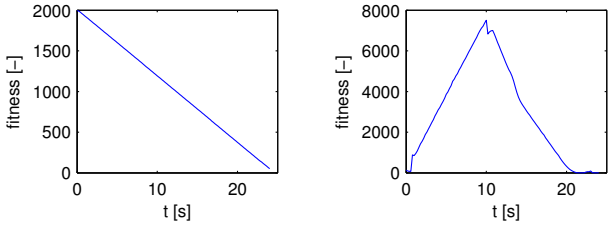

(a) Leader (b) Follower 1

Fig. 5. Objective functions of robots in simulation in Fig. 4.

and returns back to its desired position. The temporary increase of values of the objective function of the follower 1 is shown in Fig. 5. The leader's objective function is constantly decreasing as it approaches to the target region without any proximity to obstacles.

In the simulation in Fig. 6, the formation is flying through a door inside a room. Then the formation is flying over an obstacle, which is followed by an avoidance manoeuvre under the second obstacle. The complex plan of flying through both doors and avoiding both obstacles is composed together in one optimization process.

Finally, graphs in Fig. 7 present Euler angles, the total thrust force and components of moment $[m_x, m_y, m_Z]$ along axes of the body-fixed frame for a follower following a leader, which is leading the formation in an environment with obstacles.

5. CONCLUSION

A motion planning and formation control approach designed for teams of MAVs is presented in this paper. A

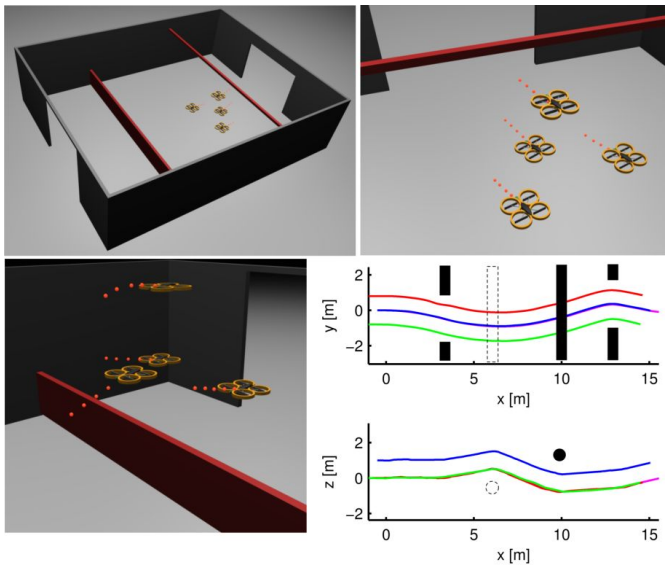

Fig. 6. Snapshots of the formation driving in an office environment with depicted trajectories of all robots.

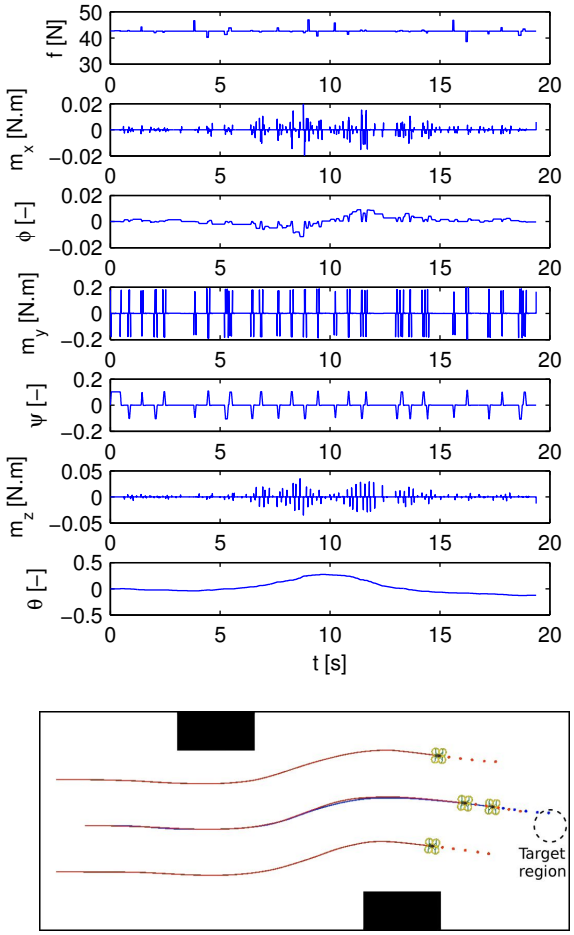

Fig. 7. Control inputs and euler angles of a follower flying behind and above the leader in the simulation shown in the last picture.

novel MPC methodology is introduced with integrated trajectory planning and obstacle avoidance functions that ensure collision free trajectories for the entire formations as well as for each of the followers. The proposed method has been verified in numerous simulations in real world environments. The ability of autonomous adaptation of the formation shape enforced by the environment, recovery of the formation driving mechanism from a failure of one of the follower and inter vehicle collision avoidance were tested.

REFERENCES

Barfoot, T.D. and Clark, C.M. (2004). Motion planning for formations of mobile robots. *Robotics and Autonomous Systems*, 46, 65–78.

Chao, Z., Zhou, S.L., Ming, L., and Zhang, W.G. (2012). Uav formation flight based on nonlinear model predictive control. *Mathematical Problems in Engineering*, 2012(1), 1–16.

Das, A., Fierro, R., Kumar, V., Ostrowski, J., Spletzer, J., and Taylor, C. (2003). A vision-based formation control framework. *IEEE Transactions on Robotics and Automation*, 18(5), 813–825.

Defoort, M. (2010). Distributed receding horizon planning for multi-robot systems. In *IEEE International Conference on Control Applications (CCA)*, 1263 –1268.

Kumar, V. and Michael, N. (2012). Opportunities and challenges with autonomous micro aerial vehicles. *Int. Journal of Robotic Research*, 31(11), 1279–1291.

Lee, T., Leoky, M., and McClamroch, N. (2010). Geometric tracking control of a quadrotor uav on se(3). In *49th IEEE Conference on Decision and Control (CDC)*.

Liu, C., Chen, W.H., and Andrews, J. (2011). Piecewise constant model predictive control for autonomous helicopters. *Robotics and Aut. Syst.*, 59(78), 571 – 579.

Liu, Y. and Jia, Y. (2012). An iterative learning approach to formation control of multi-agent systems. *Systems & Control Letters*, 61(1), 148 – 154.

Min, H.J. and Papanikolopoulos, N. (2012). Robot formations using a single camera and entropy-based segmentation. *J of Intelligent and Robotic Syst.*, (1), 1–21.

No, T.S., Kim, Y., Tahk, M.J., and Jeon, G.E. (2011). Cascade-type guidance law design for multiple-uav formation keeping. *Aerospace Science and Technology*, 15(6), 431 – 439.

Saska, M., Mejia, J.S., Stipanovic, D.M., Vonásek, V., Schilling, K., and Preucil, L. (2013). Control and navigation in manoeuvres of formations of unmanned mobile vehicles. *European Journal of Control*, 19(2), 157 – 171.

Sira-Ramirez, H. and Castro-Linares, R. (2010). Trajectory tracking for non-holonomic cars: A linear approach to controlled leader-follower formation. In *IEEE Conf. on Decision and Control (CDC)*.

Stipanović, D.M., Hokayem, P.F., Spong, M.W., and Šiljak, D.D. (2007). Cooperative avoidance control for multi-agent systems. *Journal of Dynamic Systems, Measurement, and Control*, 129, 699–707.